Journal of Applied Polymer Science

In situ studies of bovine serum albumin adsorption onto functionalized polystyrene latices monitored with a quartz crystal microbalance technique

Manel Beragoui,[1] Chadlia Aguir,[2] Mohamed Khalfaoui,[1] Eduardo Enciso,[3] Maria José Torralvo,[3] Laurent Duclaux,[4] Laurence Reinert,[4] Marylène Vayer,[5] Abdelmottaleb Ben Lamine[1]

[1]Unité de Recherche de Physique Quantique, Faculté des Sciences de Monastir, Université de Monastir, Monastir, Tunisia
[2]Unité de Recherche de Chimie Appliquée et Environnement, Faculté des Sciences de Monastir, Université de Monastir, Monastir, Tunisia
[3]Departamento de Química Física I, Facultad de Ciencias Químicas, Universidad Complutense, Madrid 28040, Spain
[4]Laboratoire de Chimie Moléculaire et Environnement, Université de Savoie, France
[5]Centre de Recherche sur la Matière Divisée, 1b Rue de la Férollerie, Orléans 45071, France
Correspondence to: M. Khalfaoui (E-mail: mohamed_khalfaoui@yahoo.com)

ABSTRACT: The adsorbability of bovine serum albumin (BSA) onto poly(styrene-*co*-itaconic acid) (PS–IA), poly(styrene-*co*-hydroxyethyl methacrylate) (PS–HEMA), poly(styrene-*co*-acrylic acid) (PS–AA), and poly(styrene-*co*-methacrylic acid) (PS–MAA) latices were investigated with a quartz crystal microbalance. The amount adsorbed onto the functionalized latices, except for PS–MAA, was greater than that adsorbed onto polystyrene (PS) latex. To explain this result, two kinds of interaction forces were considered, hydrogen bonding and hydrophobic interactions, whereas electrostatic interaction was assumed to be small. When comparing the two extremes of hydrophobic interaction and hydrogen bonding, the latter was stronger. The corrected adsorption mass suggested that the BSA molecules were adsorbed onto the PS–MAA latex in a side-on mode. However, in the case of the PS, PS–IA, PS–HEMA, and PS–AA latices, the BSA molecules were probably adsorbed in multiple layers. The presence of the BSA in the latex particle surface was verified by attenuated total reflectance/Fourier transform infrared spectroscopy and atomic force microscopy. © 2015 Wiley Periodicals, Inc. J. Appl. Polym. Sci. **2015**, *132*, 42055.

KEYWORDS: adsorption; copolymers; proteins; surfaces and interfaces

accepted 29 January 2015
DOI: 10.1002/app.42055

INTRODUCTION

There are currently several means of attaching biological ligands to the microspheres used as solid-phase supports in immunological tests and assays; these include adsorption to plain polymeric microspheres and attachment to surface-functionalized microspheres. The original method for the attachment of proteins to polymeric microspheres was passive adsorption. Because of the simplicity and flexibility of this method, it is still widely used today. Understanding the mechanism and processes involved when a protein interacts at the solid–liquid interface is essential for a number of medical and biochemical applications.[1–4]

With this objective, many academic studies[4–10] have been performed to determine the many complex phenomena involved when such biomolecules interact with polymer latices,[11] especially with regard to bovine serum albumin (BSA). Hitherto, polystyrene (PS) latices have been used as soap-free latex substrates for proteins in many investigations. That is because the PS latex is stable and monodisperse. However, with only PS latex, it is not sufficient to study the relation between the amounts adsorbed and the surface properties of the latices.

From this point of view, various functionalized PS latexes bearing carboxylic, sulfonate, aldehyde, or amino groups to provide immobilization of the proteins have been reported.[12–15] As a result, it is known that there is considerable specificity and selectivity in protein adsorption. However, its mechanism is still not completely understood. On the other hand, the mechanism of protein adsorption in an aqueous solution onto polymer latices has been studied by many different methods. For instance, Suzawa *et al.*[16] extensively investigated the adsorption of BSA by means of UV spectroscopy and carbodiimide methods. Wangkam *et al.*[17] analyzed it by surface plasma resonance. However, these methods exhibit some deficiency in the process of experimental operation. Some are sensitively limited, and others

cannot provide real-time information on protein adsorption behavior. At present, the quartz crystal microbalance (QCM) technique may be a comparatively good and effective method for the *in situ* monitoring of protein adsorption. The QCM method has been successfully used for the investigation of the adsorption process at the solid–solution interface.[18–20]

The ultimate goal of this study was to explore the adsorption phenomenon of protein on a solid surface. For this reason, monodisperse and stable soap-free latices, that is, with PS as a homopolymer and poly(styrene-*co*-itaconic acid) (PS–IA), poly(styrene-*co*-methacrylic acid) (PS–MAA), poly(styrene-*co*-acrylic acid) (PS–AA), and poly(styrene-*co*-hydroxyethyl methacrylate) (PS–HEMA) as copolymers, were prepared. BSA, a protein that has been widely used in a number of research studies, was chosen as model protein to examine its adsorption. Furthermore, to obtain a direct and comprehensive understanding of the protein behavior on the PS and its acrylate copolymers, a QCM device was used to monitor *in situ* the interaction of BSA and these polymers latices.

EXPERIMENTAL

Materials

BSA (Sigma Chemical Co., crystallized and lyophilized BSA, 96%) was used without further purification.

An acetic buffer solution, a mixture of sodium acetate and acetic acid (both from Sigma Chemical Co.), was used.

Styrene (Sigma Aldrich, 99%) was purified with a 0.1*M* sodium hydroxide solution to remove inhibitors. Acrylic acid (Aldrich, 99%), itaconic acid (Aldrich, 99%), methacrylic acid (Aldrich, 99%), 2-hydroxyethyl methacrylate (Aldrich, 97%), and potassium persulfate (Sigma Aldrich, 99%) were used without further purification. All other chemicals were analytical grade. Distilled water was used in all of the experiments.

Preparation and Characterization of the Microsphere Latices

Latex particles were prepared by the surfactant-free emulsion polymerization (PS) or copolymerization of poly[styrene-*co*-hydroxyethyl methacrylate], PS–HEMA, poly[styrene-*co*-acrylic acid], PS–AA, poly[styrene-*co*-methacrylic acid], PS–MAA and poly[styrene-*co*-itaconic acid], PS–IA according to procedures similar to those developed by Carbajo *et al.*[21]

The average particle diameters (D_n) of these microspheres were determined by field emission scanning electron microscopy (JEOL 6335F electron microscope operating at 12 μA and 5 kV). The specific surface area (S_{BET}) values of PS and its copolymers were calculated from N_2 sorption isotherms by the multipoint Brunauer–Emmett–Teller method. N_2 sorption was conducted at 77 K with an ASAP 2020 instrument (Micromeritics). The surface charge density (σ) and the number density of the surface functional groups (N_c) were determined by potentiometric and conductometric titrations, respectively. A Suntex SC-17A conductivity meter (Taiwan) was used for titration.

Evaluation of Adsorption Isotherms with QCM

The QCM setup consisted of the electrode, the QCM instrument (model QCM 200), a crystal holder, and a house-customized reactor made of Teflon. AT-cut quartz crystals [fundamental resonance frequency = 5 MHz, characteristic frequency shift ($\Delta f/\Delta m$) = 0.057 Hz/(ng/cm^2), and apparent area of electrode = 1.26 cm^2) was used as electrode. Mass added to or removed from the crystal or electrode surface induced a shift in the crystal resonance oscillation frequency. In the ideal case, the mass–frequency relationship is described by the Sauerbrey equation:[22]

$$\Delta f = -C_f \cdot \frac{\Delta m}{A} \quad (1)$$

where Δf (Hz) is the frequency shift, A is the sensible surface area of quartz (cm^2), Δm is the additional mass deposited on the quartz (μg/cm^2), and C_f is the calibration constant when the resonance frequency is equal to 5 MHz (56.6 Hz μg^{-1} cm^2).

After the gold surface of the QCM electrode was cleaned with piranha solution, a thin layer of polymer solution (10 mg/mL in chloroform) was spin-coated at 3000 rpm for 1 min onto the gold quartz crystal surface. The coatings were finally overnight drying at 67°C *in vacuo* to consolidate the coupling of the prepared latex and gold surface. The formation of the polymer film was also observed by the monitoring of the QCM signal change. Before and after the microsized polymer coating modification, the frequency of the quartz crystal was measured, and the thicknesses of the thin polymer film coatings were estimated from the amounts of deposited latex particles. The QCM crystal holder was immersed in a reactor filled with 35 mL of a buffer solution, and the solution was stirred with a magnetic stirrer. After stabilization of the QCM frequency change, which usually took around 2 h, 1 mL of concentrated BSA (0.5 mg/mL) was injected with syringe while the solution was stirred. The reported concentration of BSA was the final concentration in the reactor.

Attenuated Total Reflectance (ATR)/Fourier Transform Infrared (FTIR) Spectroscopy

ATR–FTIR measurements were performed on a Nicolet iS10 Fourier transform infrared spectrometer coupled with an ATR accessory (Thermo Scientific). Sixty-four scans were performed with a resolution of 4 cm^{-1}.

Atomic Force Microscopy (AFM)

A Nanoscope III (Digital Instruments Corp.) was used in tapping mode for the topographic characterization of the adsorbed film. A resonance frequency of 300 kHz and a scanning speed of 1 Hz were used for topographic imaging. The instrument was operated at room temperature in air. The preparation of the adsorbed albumin film was carried out by immersion of the sample in the BSA solution (70 μg/mL) for 1 h at room temperature. After immersion, the sample was rinsed with buffer solution to remove unbound protein.

RESULTS AND DISCUSSION

Characterization of the Latex Particles

Figure 1 displays scanning electron microscopy (SEM) micrographs of the PS, PS–AA, PS–IA, PS–MAA, and PS–HEMA particles. It is worth noting that particles were spherical, and their diameters showed a low polydispersity. The number-average diameter of the particles (D_n) and the polydispersity index (PDI = D_m/D_n, where D_m is the mass-average diameter) of the

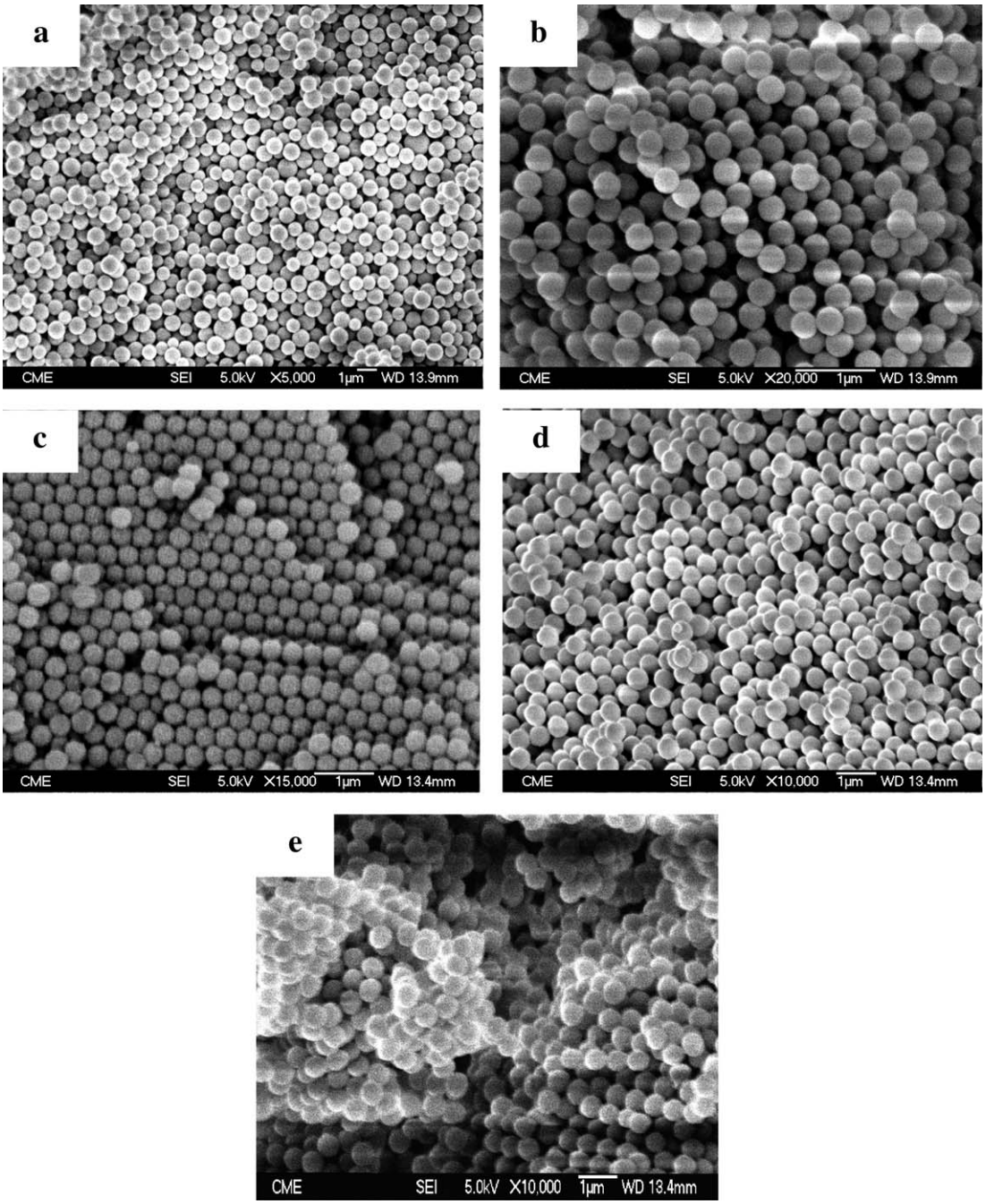

Figure 1. SEM micrographs of the investigated particles: (a) PS–MAA, (b) PS, (c) PS–IA, (d) PS–HEMA, and (e) PS–AA.

particles were calculated with SEM data from D_n and D_m as follows:

$$D_n = \frac{\sum N_i D_i}{\sum N_i} \quad (2)$$

$$D_m = \frac{\sum N_i D_i^4}{\sum N_i D_i^3} \quad (3)$$

where D_i is the diameter of individual particles and N_i is the number of particles corresponding to the diameters. As shown in Table II, D_n increased from 339 nm (PDI = 1.003) to 653 nm (PDI = 1.007) in the order PS–MAA < PS–HEMA < PS–AA < PS–IA < PS. Indeed, less hydrophilic acrylate monomers showed a better copolymerization with styrene, and that indicated a rise in the solubility of the polymer oligomers and an increase in the number of polymer particle nuclei; this finally led to smaller particle sizes. In the case of more hydrophilic monomers (e.g., itaconic acid), the copolymerization was complicated by the different monomer reactivity ratios and solubilities, and the nuclei appeared when rich styrene oligomers were not stable. This led to diameter sizes that were slightly smaller than those of the styrene latices.

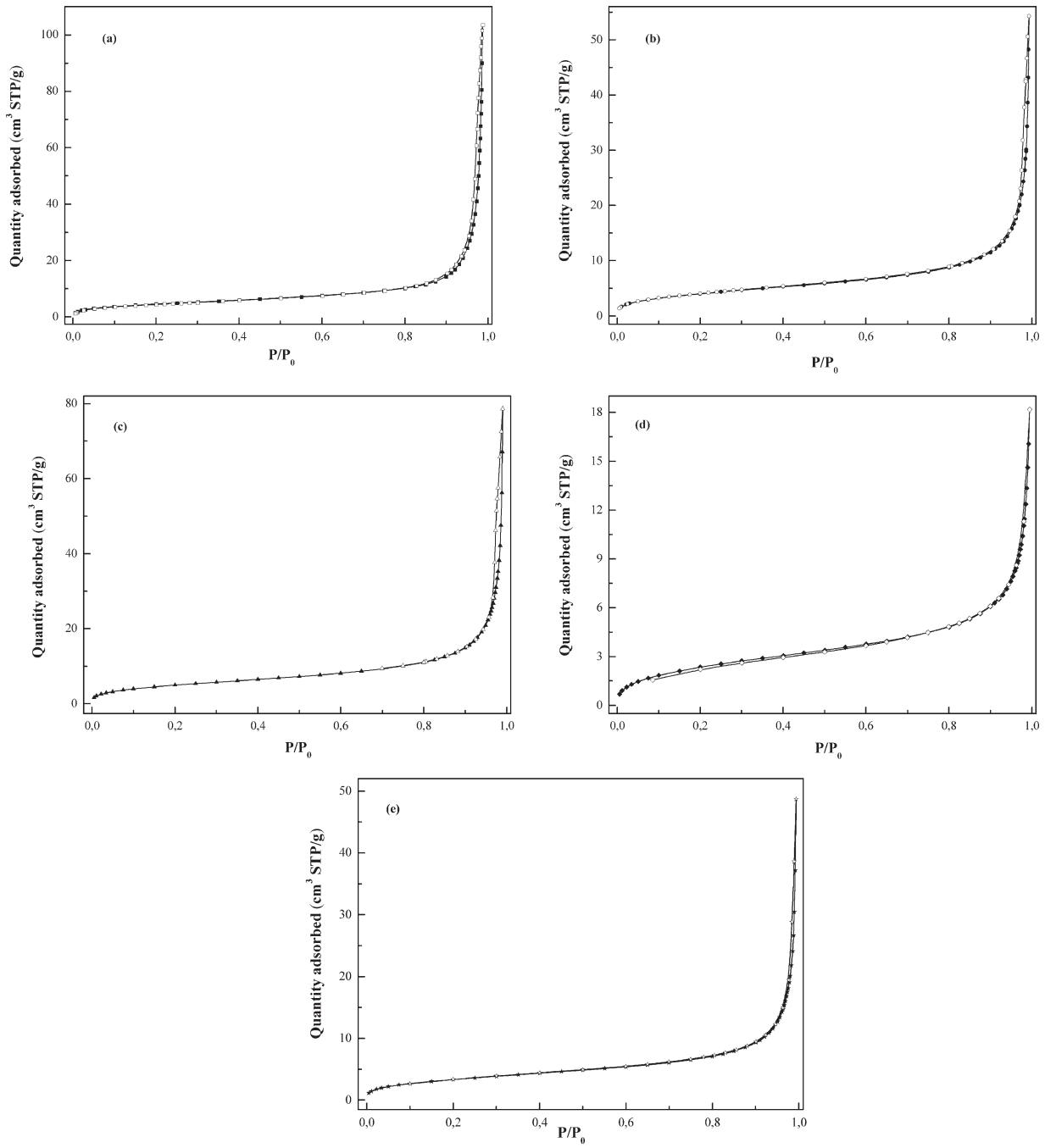

Figure 2. Adsorption–desorption isotherms for the different latexes: (a) PS–HEMA, (b) PS–AA, (c) PS–MAA, (d) PS, and (e) PS–IA (filled symbols, adsorption; empty symbols, desorption). P is the nitrogen pressure and P_0 is its saturated vapour pressure.

Table I. Molar Compositions of the Feed Polymerization Mixtures

Sample	n_s	n_{CM}	$n_{KPS} \times 10^3$	Temperature (°C)
PS	2.27	—	2.90	69
PS-MAA	1.53	0.11	2.20	76
PS-AA	1.48	0.11	2.30	76
PS-IA	1.53	0.11	2.30	76
PS-HEMA	0.30	0.041	0.45	76

n_s, molar number of styrene; n_{CM}, molar number of the comonomer; n_{KPS}, molar number of the potassium persulfate initiator.

Table II. Characteristic Parameters of the Latex Particles

Sample	D_n (nm)	PDI	S_{BET} (m^2/g)	Comonomer (wt %)
PS	653	1.007	9.00	—
PS-MAA	339	1.002	18.60	5.60
PS-AA	404	1.005	15.10	5.00
PS-IA	508	1.004	12.60	8.50
PS-HEMA	342	1.003	17.00	12.50

Table III. Maximum Adsorbed Quantities of BSA with Various Polymer Lattices

Sample	$Q_{\sigma\ max}$ (μg/cm^2)	$Q_{\sigma\ max\ real}$ (μg/cm^2)[a]
PS-MAA	0.715	0.325
PS	2.280	1.036
PS-AA	7.645	3.475
PS-HEMA	14.332	6.514
PS-IA	25.666	11.666

[a] Real maximum adsorbed amount of BSA.

S_{BET} is important for the industrial process and chemical reaction. Even with the same material that has the same weight and volume, the surface activity and adsorption volume change according to S_{BET}. So it is important to measure S_{BET} to evaluate the activity and adsorption capacity of materials. (e.g., catalysis and adsorbent). The surface areas of all of the samples under study were evaluated by with a nitrogen adsorption–desorption method. All of the materials yielded a type IV isotherm (Figure 2). A summary of the results generated from the nitrogen adsorption–desorption experiments is shown in Table II. S_{BET} increases as the particle size becomes small according to the theoretical specific surface, S, expression of isolated hard spheres:

$$S = \frac{6}{\rho D}$$

where ρ is the bulk polymer density (1.05 g/cm^3 for styrene). The slightly lower values obtained by the previous equation could be understood by the presence of some microporosity.

On the basis of the results of the potentiometric titrations, with the assumption that the difference in the titration volume between the blank and latex dispersion systems corresponded to the volume of the HCl aqueous solution, which was used for the titration of surface groups of the latex particles at some pH values, we were able to determine the σ values of the latexes with the following equation:

$$\sigma = \frac{FC}{Sm}(V_s - V_B) \quad (4)$$

where F is the Faraday constant, m is the mass of the sample, C is the concentration of the HCl solution, V_S is the volume of HCl added to the sample, and V_B is the volume of HCl added to the blank. Figure 3 shows the results of the σ measurements. All of these latices had a negative charge derived from the dissociation of the acid acrylate comonomers and/or decomposed initiator fragments. Up to a pH of about 5, $-\sigma$ for the carboxylated latices was almost equal to those of the PS and PS–HEMA latices because the carboxyl groups hardly dissociate in this pH region. However, at pHs higher than about 5, $-\sigma$ for each latices increased with increasing pH. This tendency was greater for the carboxylated latexes than for the PS and PS–HEMA latices (2-hydroxyethyl methacrylate has no ionized group). This may have arisen from the dissociation of weak acid groups of the latex surface. For this result, the following explanations were possible

1. As 2-hydroxyethyl methacrylate was more hydrophilic than styrene, water-soluble initiator fragments may have been incorporated more into the PS–HEMA latex than into the PS latex. Therefore, it seemed that weak acid groups existed more on the PS–HEMA latex than on the PS latex.
2. Weak acid groups may have formed by hydrolysis of 2-hydroxyethyl methacrylate during the polymerization.
3. The σ values (except in the acidic region) for the carboxylated latices were proportional to the amount of comonomer used in their copolymerization. The differences in the surface properties of these latices may have greatly affected the BSA adsorption.

The results reported here are in agreement with other reported studies in the literature.[23,24]

Table IV. Thicknesses of the Adsorbed BSA after and before Rinsing onto Various Polymer Latexes

Sample	d_f before rinsing (nm)	d_f after rinsing (nm)
PS	16.216	4.55
PS-IA	182.546	76.979
PS-HEMA	101.934	52.852
PS-AA	54.374	32.370
PS-MAA	5.085	4.98

Table V. Frequency Shifts Due to the Roughness of the Used Latex Polymers

Sample	$-\Delta F$ (kHz)
PS-HEMA	2.142
PS-IA	1.376
PS-AA	1.298
PS	0.773
PS-MAA	0.740

Adsorption of BSA.

It has been shown that proteins have no net charge at their isoelectric point (IEP); therefore, the maximum amount of

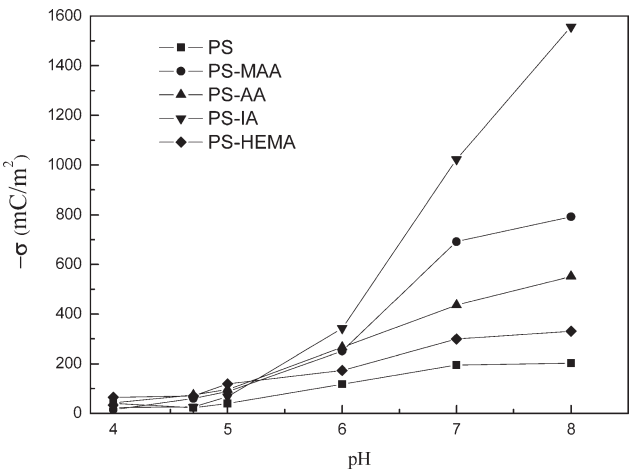

Figure 3. σ values for various polymer lattices as a function of pH.

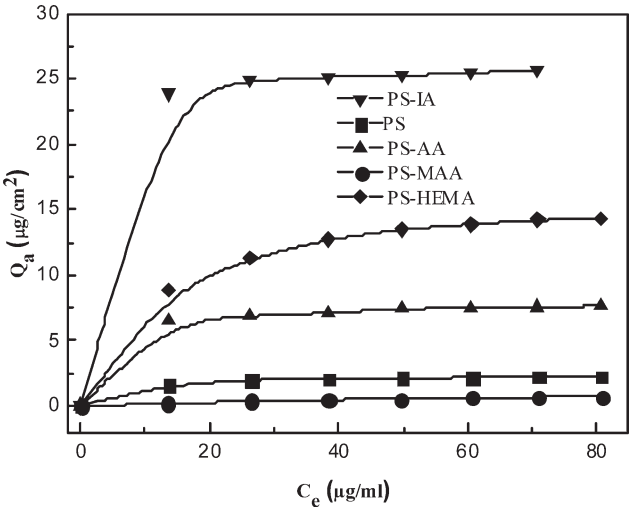

Figure 4. Adsorption isotherms of BSA onto various polymer latices.

adsorption from an aqueous solution is observed at its IEP.[25–30] Below or above their IEP values, proteins are charged positively or negatively, respectively. Therefore, they are more hydrated; this increases their stability and solubility in the aqueous phase and indicates low adsorption. Thus, it is productive to study protein adsorption at its IEP. To do so, we chose to investigate adsorption of BSA onto PS and its acid copolymers at a pH of 4.7.

On the basis of the frequency changes in the equilibrium state of the adsorption, the amount of protein adsorbed (Q_a) onto each coated electrode was calculated with eq. (1). The results are shown in Figure 4, where the adsorption amounts are plotted against the protein equilibrium concentration (C_e) in acetic buffer. In all of the latex polymer systems, Q_a increased sharply when the protein solution was injected into the acetic buffer and then reached a plateau.

The maximum adsorption amounts of BSA ($Q_{a\ max}$) for PS, PS–IA, PS–AA, PS–MAA, and PS–HEMA were 2.280, 25.666, 7.645, 0.715, and 14.332 $\mu g/cm^2$, respectively (Table III). These results show a markedly different adsorption behavior toward the polymer surface. The large value for PS–IA and the rather small value for PS–MAA were attributed to the different kinds of interactions between the polymer and BSA. These values were similar to those measured with the QCM method and reported in literature.[31,32] The adsorption mass of BSA onto the same hydrophobic surface as in this study was reported as 1.9 $\mu g/cm^2$.[31] However, the results obtained by the QCM method were greater by factor of about 10 compared with those found by other common methods. Indeed, ellipsometry for the adsorption mass on tantalum oxide gave a value of 0.332 $\mu g/cm^2$.[33] The microbiuret method gave a value of 0.2 $\mu g/cm^2$ for the adsorption mass onto PS and a styrene/2-hydroxyethyl methacrylate copolymer.[9] Neutron reflectivity measurements gave a value of 0.3 $\mu g/cm^2$ for the adsorption mass on a hydrophilic silica–water interface.[34] Several factors can be considered to account for difference in the adsorption mass measured by the QCM and other methods. In the QCM method, the measured mass includes the solvent molecules entrapped within the adsorbed layers. The frequency shift of the QCM method reflects the mass of the material adsorbed on the electrode surface and that within the macroscopic no-slip plane.[35] Therefore, the frequency changes cannot be converted into the exact mass of adsorbed protein through the Sauerbrey equation.

As mentioned previously, in the QCM technique, the calculated adsorbed mass corresponds to the sum of the dry protein and the trapped solvent. When we assumed a total mass versus dry mass ratio of 2.2,[36,37] the real adsorbed BSA was in the range 0.325–11.666 $\mu g/cm^2$ (Table III), and this value was considerably higher than that found in previous works.[4,24] According to some authors, the BSA monolayer superficial concentration limit varies between 0.14 and 0.30 $\mu g/cm^2$ for a side-on configuration and between 0.23 and 0.90 $\mu g/cm^2$ for an end-on configuration.[38–44] From the limit of these two configurations and the corrected adsorption mass in the case of the PS–MAA latex, the BSA molecule adsorbed onto this latex in a monolayer side-on configuration. However, our corrected adsorption masses for PS–IA, PS–AA, PS–HEMA, and PS (11.666, 3.475, 6.514 and 1.036 $\mu g/cm^2$, respectively) were greater than those of these two configurations. Therefore, some explanations are possible, and they include the flexibility of the BSA molecules, the tilting of protein molecules due to the asymmetry of the charge distribution, or multilayer formation.[2,45] The calculation of the adsorbed layer thickness will clearly express this large adsorbed amount.

The coupled water sensed by the QCM method must be contained within the adsorbed protein film. At high coverage, that is, at or close to saturation where most water in the protein film is coupled, it is reasonable to represent the protein film with an effective hydrodynamic thickness (d_f) and an effective density of the adsorbed layer ($\rho_{effective}$). The effective thickness can be directly expressed with the mass uptake (Δm) estimated from Δf [according to eq. (1)] and the density of bovine serum albumin (ρ_{BSA}) via the following relation:[40,46]

$$d_f = \frac{\Delta m}{\rho_{effective}}; \rho_{BSA} = 1.406 g/cm^3 \quad (5)$$

The effective thicknesses, determined by the QCM method, of the adsorbed BSA layer were 16.216, 182.546, 101.934, 54.374,

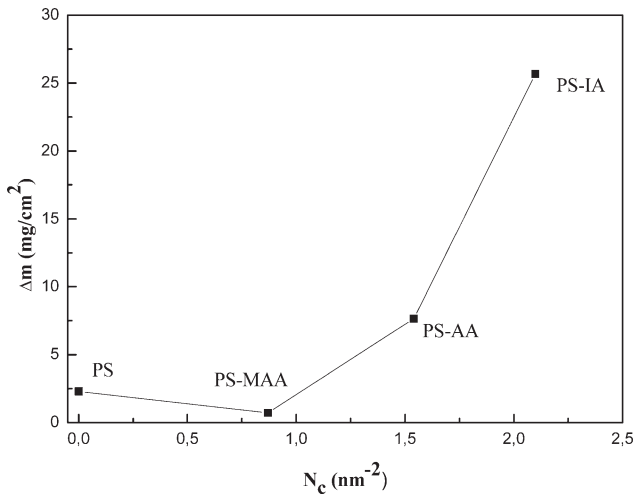

Figure 5. Adsorption of BSA onto different latex particles as a function of the surface density of carboxylic groups.

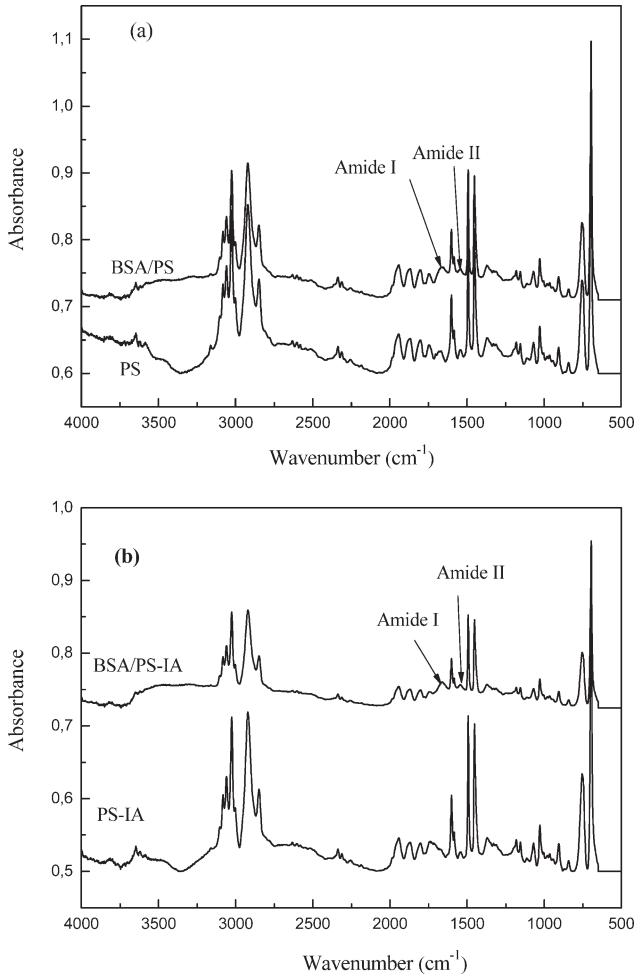

Figure 6. ATR–FTIR spectra before and after BSA adsorption onto (a) PS and (b) PS–IA.

and 5.085 nm for PS, PS–IA, PS–HEMA, PS–AA, and PS–MAA, respectively (Table IV). These thickness values obtained after rinsing by the buffer solution indicated that BSA could adopt multilayer adsorption onto PS, PS–IA, PS–HEMA, and PS–AA. However, in a multilayer system, the protein will be weakly attached to the surface, and rinsing will drag a significant part of the molecules under these conditions.[39] In our case, rinsing led to a very large decrease in the adsorbed mass and suggested the existence of a multilayer.

The existence of a dimer or oligomer provides another possibility because commercially available BSA is composed of 90% monomer, 10% dimer, and a small amount of oligomer. This type of protein molecule increases the adsorbed amount itself; it also facilitates the formation of a multilayer. Peula and De Las Nieves[45] reported that the adsorbed amount of oligomeric BSA was 5.5 mg/m^2.

The d_f values obtained after rinsing for the PS, PS–IA, PS–HEMA, PS–AA, and PS–MAA latices were 4.55, 76.979, 52.852, 32.370, and 4.98 nm, respectively (Table IV). The approximate ellipsoid dimensions of BSA were 14 × 4 × 4 nm^3.[38,47] With the d_f values after rinsing and the dimensions of the BSA molecules in PS and PS–MAA latices, the BSA molecules probably adsorbed onto these latices in a side-on monolayer. On the other hand, the d_f values after rinsing for PS–IA, PS–HEMA, and PS–AA (76.979, 52.852, and 32.370 nm, respectively) were greater than those for the PS and PS–MAA latices. Because these thicknesses exceeded 14 nm, the consideration of a multilayer adsorption was necessary.

Contribution of the Latex Surface to Adsorption. As described in the Characterization of the Latex Particles section, we found that the surface properties of the latices were very different from one another. Accordingly, it seems to be interesting to discuss the effect of the latex properties on the protein adsorption.

At pH 4.7 (the IEP of BSA), because the electrostatic repulsion between BSA and the latex was negligible, the BSA molecules could adsorb onto these latices easily by van der Waal's forces, hydrogen bonding (which mainly affects the adsorption onto functionalized latex), or hydrophobic interactions (which mainly affected the adsorption onto the PS latex). Also, at this pH, the plateau values of the amounts adsorbed onto the functionalized copolymer (PS–IA, PS–AA, and PS–HEMA) latices (Figure 4) were considerably greater than that onto the PS latices with the exception of PS–MAA. These latices contained surface-functional groups derived from the comonomer. Therefore, those surfaces were more hydrophilic than that of the PS latex. This may have led to the same decrease in the amount adsorbed as the PS–AA latex, which was more hydrophilic than the PS latex. However, on the contrary, the amounts adsorbed increased. This may have been due to hydrogen-bond formation between protein molecules and functional groups on the latex surface, as Kim *et al.*[48] demonstrated that hydrogen bonding between segmented copolyether–urethane–urea based on poly(-propylene glycol) and serum albumin increased the adsorbed amount. The reason for the marked low adsorption of the proteins observed on the PS–MAA surface was mainly attributed to steric repulsion in addition to the decrease in the hydrophobic interactions between the latex and the protein.[25,49–51]The previous results could be confirmed by the study of N_c as follows.

The plot of Q_a versus N_c per square nanometer is shown in Figure 5 (the PS data are also plotted; the N_c value was zero, although its σ was not zero). As the amount of carboxyl groups increased, Q_a decreased in the low-N_c region. However, above 0.9 carboxyl groups per square nanometer, Q_a began to increase. According to the literature,[2] the increases in N_c per square nanometer results in a decreased amount of hydrophobically adsorbed proteins and an increased Q_a by hydrogen bonding. On the basis of these results, we concluded that the hydrophobic interactions were dominant in the low-N_c region, whereas the hydrogen-bonding interactions were dominant in the high-N_c region.

When comparing the two extremes, PS (maximum hydrophobic interactions) and PS–IA (maximum hydrogen binding), we found that the latter had a large Q_a value. We concluded in this research, in contrast to other works, that the hydrogen bonding was stronger than the hydrophobic interactions. Indeed, Suzawa and Shirahama[24] stated that the adsorbed amount was in the following order: High carboxylated < Low carboxylated < PS.

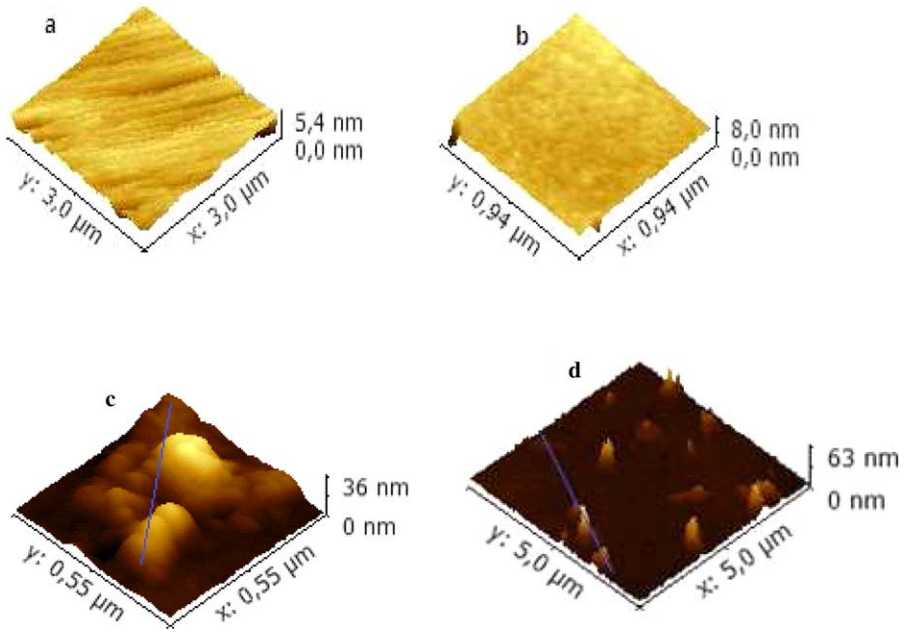

Figure 7. Comparison of the substrate topographical images without and with adsorbed BSA: (a) PS without BSA, (b) PS–IA without BSA, (c) PS with BSA, and (d) PS–IA with BSA. [Color figure can be viewed in the online issue, which is available at wileyonlinelibrary.com.]

However, their highly carboxylated microspheres were high enough so their results were different from ours.

On the other hand, there were several effects of roughness, from a simple increase in the surface area to more complex effects related to changes in the interaction between the protein and the surface. In this study, a quantitative measure of roughness was not obtained, but the connection between the roughness and an excess frequency shifted (Table V). As demonstrate in the literature, the rougher surface resulted in more trapped water; this, in turn, also shifted the resonance frequency down to the sensor.[31,52,53] From an experimental point of view, the frequency shifts found in this study were 0.740, 0.773, 1.298, 1.376, and 2.142 kHz in PS–MAA, PS, PS–AA, PS–IA, and PS–HEMA, respectively (Table V). On the basis of the obtained results, some tentative conclusions can be given. The roughness surface increased in the order of PS–MAA < PS < PS–AA < PS-IA < PS–HEMA. This difference could be explained by the chemical groups on the latex surfaces. The adsorbed quantity of BSA increased with the surface roughness with the exception of PS–HEMA. This contrast between the two forms of latices (PS–IA and PS–HEMA) could be explained from the different microscopic structures between PS–IA and PS–HEMA and the linkage modes of adsorbed molecules on PS–IA and PS–HEMA.

Visualization of the Adsorbed BSA. Generally, a protein ATR–FTIR spectrum displays two major peaks, both of them associated with the peptide band. The higher one appears at 1650 cm^{-1} (amide I band), whereas a second smaller one is observed at 1524 cm^{-1} (amide 2 band).[54] The spectra of the adsorbed BSA onto the PS and PS–IA surface are shown in Figure 6(a,b). These spectra demonstrated that the adsorption of BSA onto the PS and PS–IA surfaces was successful because the ATR–FTIR spectra of the PS–BSA and PS–IA–BSA showed the presence of the characteristic BSA absorption bands. These were located in the same spot for all of the used polymers (results not shown). The higher one was encountered between 1655 and 1650 cm^{-1}, and the second one was located at 1539 cm^{-1}.

IR analysis not only strongly confirmed the adsorption of BSA on the studied support, but it also indicated that no obvious change occurred in the polymer groups in the process of BSA adsorption; namely, BSA adsorption on the microsphere latices was a physical adsorption process, which was in good agreement with the literature.[8,55]

To obtain additional information regarding the surface characteristics of the investigated samples, AFM analyses were performed to determine the surface topography, which could also influence the protein adsorption. The AFM images of the PS and PS–IA are shown in Figure 7. As shown, the root mean square surface roughness of the polymer films on the surface of the gold-coated substrate were approximately 0.46 nm for PS and 0.59 nm for PS–IA (Figure 7). The morphologies of the PS–IA were slightly rougher than that of the PS sample. This difference could be explained by consideration of the chemical groups on the latex surfaces. These results were also supported by QCM measurements, as discussed previously.

A comparison of the topographical images before and after BSA adsorption (Figure 7) allowed us to see that the surface features of the bare surface (e.g., polishing scratches) became invisible; this suggested that the protein layer covered the whole surface area. Furthermore, the structure of the BSA aggregates could be clearly identified. These aggregates presented, in general, a diameter of about 43–290 nm in all of the five coatings, and this was in agreement with previous studies.[56]

Another conclusion that could be drawn from the results shown in Figure 8 was that the height of the adsorbed BSA layer was approximately 4.55–20.54 nm for PS and 4–54.63 nm for PS–

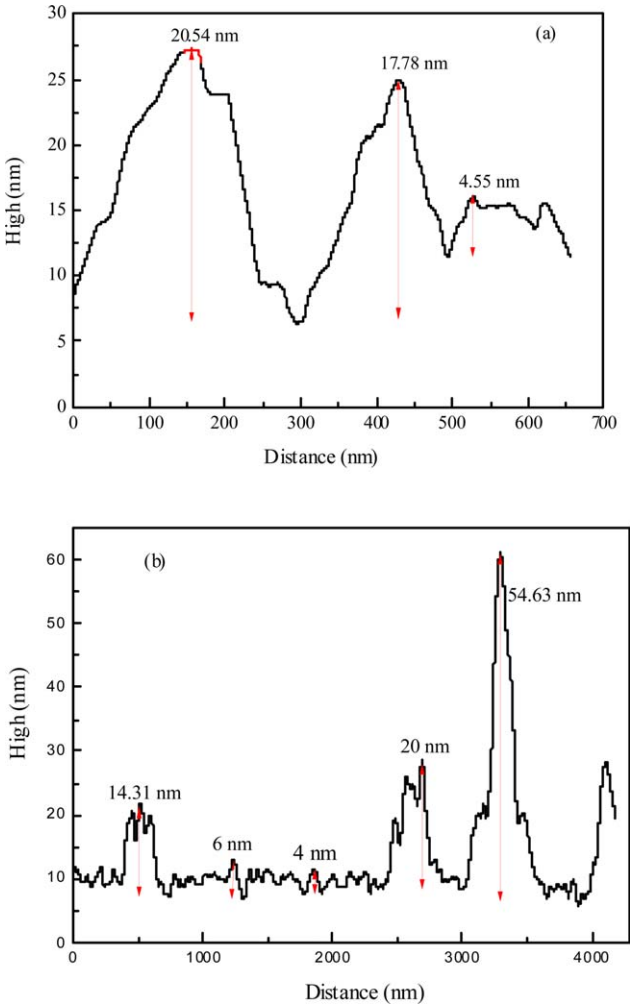

Figure 8. Topographies of the selected profiles: (a) BSA/PS and (b) BSA/PS–IA. [Color figure can be viewed in the online issue, which is available at wileyonlinelibrary.com.]

IA. These values were in qualitative agreement with those obtained with the QCM technique and were compatible with the molecular dimensions of the BSA molecules (ellipsoid configuration), which formed a monolayer or a multilayer. Similar results to these were found for the PS–AA, PS–MAA, and PS–HEMA latexes (results not shown).

CONCLUSIONS

BSA adsorption onto hydrophilic (PS–MAA, PS–AA, PS–IA, and PS–HEMA) and hydrophobic (PS) polymer surfaces was investigated with the QCM technique. On the basis of the adsorption isotherm data, the $Q_{a\ max}$ values of each polymer were obtained. The $Q_{a\ max}$ value of BSA increased in the following order: PS–MAA < PS < PS–AA < PS–HEMA < PS–IA. The reason for the marked low adsorption onto the PS–MAA surface was attributed to steric repulsion and the decrease in the hydrophobic interactions between the latex and the protein. Furthermore, the corrected adsorption mass was in the range 0.325–11.66 $\mu g/cm^2$. From this result, it was suggested that the BSA molecules adsorbed onto PS–MAA in a monolayer side-on configuration. However, the large adsorbed amounts of BSA onto PS, PS–AA, PS–HEMA, and PS–IA suggested the existence of a multilayer adsorption. These results were confirmed by the calculation of d_f.

It is well known that the surface chemistry plays a fundamental role in protein adsorption onto latices polymers. From this point of view, the surface characteristics of the five solids were determined experimentally and used in the interpretation of the isotherm data. With the experiments of BSA adsorption onto carboxylated microspheres (PS–MAA, PS–AA, and PS–IA), the quantitative effect of surface functional groups and interactions were investigated. Hydrophobic interactions were dominant in the low-N_c region, whereas hydrogen bonding was dominant in the high-N_c region. In a comparison of the extremes of the two interactions, hydrogen bonding was stronger than hydrophobic interactions. Additionally, the BSA adsorbed amount increased with the surface roughness, except for in PS–HEMA. Indeed, this result was attributed to the different microscopic structures between PS–IA and PS–HEMA and the linkage modes of the adsorbed molecules on PS–IA and PS–HEMA.

A visualization of the BSA adsorbed onto the polymer latices surface was attempted with AFM phase imaging on all of the investigated surfaces. The results were found to be in qualitative agreement with those obtained with the QCM technique and were compatible with the molecular dimensions of the BSA molecules (ellipsoid configuration) to form a monolayer or a multilayer.

ACKNOWLEDGMENTS

Finally, the BSA adsorption onto the microsphere latex coating was confirmed by ATR–FTIR spectroscopy and AFM imaging.

REFERENCES

1. Peters, T., Jr. All about Albumin: Biochemistry, Genetics, and Medical Applications; Academic Press Inc.: San Diego, USA, **1996**.
2. Yoon, J.-Y.; Park, H.-Y.; Kim, J.-H.; Kim, W.-S. *J. Colloid Interface Sci.* **1996**, *177*, 613.
3. Recek, N.; Jaganjac, M.; Kolar, M.; Milkovic, L.; Mozetič, M.; Stana-Kleinschek, K.; Vesel, A. *Molecules* **2013**, *18*, 12441.
4. Shirahama, H.; Suzawa, T. *J. Colloid Interface Sci.* **1985**, *104*, 416.
5. Andrade, J. D. Surface and Interfacial Aspects of Biomedical Polymers; Plenum: New York, **1985**; p 15.
6. Haynes, C. A.; Norde, W. *J. Colloid Interface Sci.* **1995**, *169*, 313.
7. Okubo, M.; Azume, I.; Yamamoto, Y. *Colloid Polym. Sci.* **1990**, *268*, 598.
8. Revilla, J.; Elaiüssari, A.; Carriere, P.; Pichot, C. *J. Colloid Interface Sci.* **1996**, *180*, 405.
9. Shirahama, H.; Suzawa, T. *Colloid Polym. Sci.* **1985**, *263*, 141.

10. Okubo, M.; Yamamoto, Y.; Uno, M.; Kamei, S.; Matsumoto, T. *Colloid Polym. Sci.* **1987**, *265*, 1061.
11. Gerard, M.; Chaubey, A.; Malhotra, B. *Biosens. Bioelectron.* **2002**, *17*, 345.
12. Oenick, M. B.; Warshawsky, A. *Colloid Polym. Sci.* **1991**, *269*, 139.
13. Betton, F.; Theretz, A.; Elaissari, A.; Pichot, C. *Colloids Surf. B* **1993**, *1*, 97.
14. Amagasa, H.; Hagiya, T.; Kimura, N.; Ohtsuka, Y. *Colloids Surf.* **1985**, *13*, 295.
15. Delair, T.; Marguet, V.; Pichot, C.; Mandrand, B. *Colloid Polym. Sci.* **1994**, *272*, 962.
16. Suzawa, T.; Shirahama, H.; Fujimoto, T. *J. Colloid Interface Sci.* **1982**, *86*, 144.
17. Wangkam, T.; Srikhirin, T.; Wanachantararak, P.; Baxi, V.; Sutapun, B.; Amarit, R. *Sens. Actuators B* **2009**, *139*, 274.
18. Sener, G.; Ozgur, E.; Yılmaz, E.; Uzun, L.; Say, R.; Denizli, A. *Biosens. Bioelectron.* **2010**, *26*, 815.
19. Rickert, J.; Brecht, A.; Göpel, W. *Biosens. Bioelectron.* **1997**, *12*, 567.
20. Rickert, J.; Weiss, T.; Kraas, W.; Jung, G.; Göpel, W. *Biosens. Bioelectron.* **1996**, *11*, 591.
21. Carbajo, M. C.; Enciso, E.; Torralvo, M. *J. Colloids Surf. A* **2007**, *293*, 72.
22. Sauerbrey, G. Z. *Phys.* **1959**, *155*, 206.
23. Shirahama, H.; Suzawa, T. *Polym. J.* **1984**, *16*, 795.
24. Suzawa, T.; Shirahama, H. *Adv. Colloid Interface Sci.* **1991**, *35*, 139.
25. Shirahama, H.; Shikuma, T.; Suzawa, T. *Colloid Polym. Sci.* **1989**, *267*, 587.
26. Shirahama, H.; Takeda, K.; Suzawa, T. *J. Colloid Interface Sci.* **1986**, *109*, 552.
27. Suzawa, T.; Murakami, T. *J. Colloid Interface Sci.* **1980**, *78*, 266.
28. Suzawa, T.; Shirahama, H.; Fujimoto, T. *J. Colloid Interface Sci.* **1983**, *93*, 498.
29. Tuncel, A.; Denizli, A.; Abdelaziz, M.; Ayhan, H.; Piskin, E. *Clin. Mater.* **1992**, *11*, 139.
30. Zsom, R. L. *J. Colloid Interface Sci.* **1986**, *111*, 434.
31. Sakti, S.; Rösler, S.; Lucklum, R.; Hauptmann, P.; Bühling, F.; Ansorge, S. *Sens. Actuators A* **1999**, *76*, 98.
32. Allen, S. J.; Gan, Q.; Matthews, R.; Johnson, P. A. *Bioresour. Technol.* **2003**, *88*, 143.
33. Mora, M. F.; Wehmeyer, J. L.; Synowicki, R.; Garcia, C. D. Investigating protein adsorption via spectroscopic ellipsometry. In Biological Interactions on Materials Surfaces. Springer: US, **2009**.
34. Su, T.; Lu, J.; Thomas, R.; Cui, Z. *J. Phys. Chem. C* **1999**, *103*, 3727.
35. Rodahl, M.; Kasemo, B. *Sens. Actuators A* **1996**, *54*, 448.
36. Serro, A.; Completo, C.; Colaço, R.; Dos Santos, F.; da Silva, C. L.; Cabral, J.; Araújo, H.; Pires, E.; Saramago, B. *Surf. Coat. Technol.* **2009**, *203*, 3701.
37. Vörös, J. *Biophys. J.* **2004**, *87*, 553.
38. Anzai, J.; Guo, B.; Osa, T. *Bioelectrochem. Bioenerg.* **1996**, *40*, 35.
39. Daeschel, M. A.; McGuire, J. *Biotechnol. Genet. Eng. Rev.* **1998**, *15*, 413.
40. Höök, F.; Kasemo, B.; Nylander, T.; Fant, C.; Sott, K.; Elwing, H. *Anal. Chem.* **2001**, *73*, 5796.
41. Jackson, D. R.; Omanovic, S.; Roscoe, S. G. *Langmuir* **2000**, *16*, 5449.
42. Rezwan, K.; Meier, L. P.; Rezwan, M.; Vörös, J.; Textor, M.; Gauckler, L. *J. Langmuir* **2004**, *20*, 10055.
43. Stobiecka, M.; Hepel, M.; Radecki, J. *Electrochim. Acta* **2005**, *50*, 4873.
44. Zhang, Y.; Fung, Y.; Sun, H.; Zhu, D.; Yao, S. *Sens. Actuators B* **2005**, *108*, 933.
45. Peula, J.; De las Nieves, F. *Colloids Surf. A* **1993**, *77*, 199.
46. Iruthayaraj, J.; Olanya, G.; Claesson, P. M. *J. Phys. Chem. C* **2008**, *112*, 15028.
47. Vallée, A.; Humblot, V.; Al Housseiny, R.; Boujday, S.; Pradier, C.-M. *Colloids Surf. B* **2013**, *109*, 136.
48. Wangkam, T.; Yodmongkol, S.; Disrattakit, J.; Sutapun, B.; Amarit, R.; Somboonkaew, A.; Srikhirin, T. *Curr. Appl. Phys.* **2012**, *12*, 44.
49. Ikada, Y.; Iwata, H.; Horii, F.; Matsunaga, T.; Taniguchi, M.; Suzuki, M.; Taki, W.; Yamagata, S.; Yonekawa, Y.; Handa, H. *J. Biomed. Mater. Res.* **1981**, *15*, 697.
50. Nagaoka, S.; Takiuchi, H.; Yokota, K.; Mori, Y.; Tanzawa, H.; Kikuchi, T. *Kobunshi Ronbunshu* **1982**, *39*, 165.
51. Shirahama, H.; Tamai, H.; Sakai, I.; Suzawa, T. Nippon Kagaku Kaishi **1985**, *6*, 1285.
52. Martin, S. J.; Frye, G. C.; Ricco, A. J.; Senturia, S. D. *Anal. Chem.* **1993**, *65*, 2910.
53. Khalfaoui, M.; Nakhli, A.; Aguir, C.; Omri, A.; M'henni, M. F.; Ben Lamine, A. *Can. J. Phys.* **2014**, *92*, 1185.
54. Van Straaten, J.; Peppas, N. A. *J. Biomater. Sci. Polym. Ed.* **1991**, *2*, 113.
55. Yin, G.; Liu, Z.; Zhan, J.; Ding, F.; Yuan, N. *Chem. Eng. J.* **2002**, *87*, 181.
56. Chen, X.; Davies, M.; Roberts, C.; Tendler, S.; Williams, P.; Davies, J.; Dawkes, A.; Edwards, J. *Langmuir* **1997**, *13*, 4106.